

## STUDY OF OPTIMUM CONDITION TO BEST EFFICIENCY OF ORGANIC-INORGANIC PEROVSKITE SOLAR CELLS

Dr. Dhuha Imad. Tareq PHD\*<sup>1</sup>, Noor Khamees Hamad MS.c<sup>2</sup> and Marrwan Hisham Mohammed MS.c<sup>3</sup>

<sup>1</sup>Department of Optics, Al-Ayen University, Nasiriyah, Iraq.

<sup>2,3</sup>Department of Optometry and Optics, Al- Mustaqbal University College, 51001 Hillah, Babylon, Iraq.

Received date: 15 March 2022

Revised date: 05 April 2022

Accepted date: 25 April 2022

\*Corresponding Author: Dr. Dhuha Imad. Tareq PHD

Department of Optics, Al-Ayen University, Nasiriyah, Iraq.

### ABSTRACT

SCAPS software was used to simulate perovskite solar cells (PSCs) made of  $\text{CH}_3\text{NH}_3\text{PbBr}_3/\text{PCBM}$  in this work. Using PCE curves, the thickness of active layers (perovskites) was tuned, and then the electrical characteristics of the solar cells were derived. According to simulation findings, the best structure with active layer  $\text{MAPbBr}_3$  has characteristics of 35.38 percent,  $45.93 \text{ mA/cm}^2$ , 1.1 V, and 69.62 % for PCE,  $J_{\text{sc}}$ ,  $V_{\text{oc}}$ , and FF, respectively. Solar cell efficiency is significantly affected by temperature, with PCE reaching 35.38 % at 213 K.

### 1-INTRODUCTION

Because of its easy manufacturing technique and substantially rising photoelectric conversion efficiency (PCE) from 3.81 percent in 2009 to 22.1 percent in 2016, perovskite solar cells based on  $\text{CH}_3\text{NH}_3\text{PbX}_3$  have recently attracted a lot of interest.<sup>[1]</sup> It is critical to examine the balance between thickness and carrier diffusion length in perovskite thin films in order to achieve high-performance devices. While increasing the thickness of the perovskite absorption layer can enhance its light-harvesting efficiency, the PCE of the associated perovskite solar cell is not necessarily improved due to the electron and hole diffusion length restrictions in perovskite absorption layers. Other qualities of perovskite, such as high absorption coefficient, high carrier transmission capacity, low-temperature manufacturing, and low susceptibility to crystal defects, enhanced the likelihood of PCE solar cells being created by absorbers by 20%. The literature has provided the fundamental knowledge needed to develop this model, thanks to the relevant simulation studies.<sup>[2]</sup> The influence features of the absorber layer (thickness) and the effect of Hole Transport Material and Electron Transport Material doping on system output were investigated and assessed in this device. SCAPS is a window application program developed at the University of Ghent using laboratory windows / CVI of a national instrument. The software is organized in a series of panels that allow the user to set parameters and calculate results.<sup>[3]</sup>

### 1.2-Structure and working of perovskites

A cation is occupied on a cubooctahedral site in perovskite structures with the generic formula  $\text{ABX}_3$  (X = oxygen, carbon, nitrogen, or halogen), whereas B cation is occupied on an octahedral site (Fig 1). A and B are commonly divalent and tetravalent when utilized with  $\text{O}^{2-}$  anion. Perovskite containing halogen anions, on the other hand, cations that are monovalent and divalent at sites A and B. As illustrated in Fig. 2b, the A-site cation is  $\text{CH}_3\text{NH}_3^+$  and the B-site cation is  $\text{Pb}^{2+}$  in  $\text{CH}_3\text{NH}_3\text{PbI}_3$ . The geometric tolerance factor is used to calculate the formability of perovskite.<sup>[4]</sup> **Fig. 1**

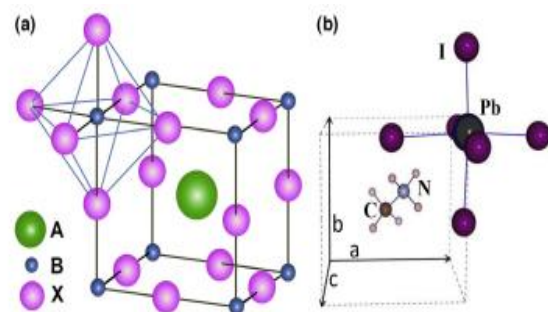


**Figure 1: (a)  $\text{BX}_6$  octahedral structure of  $\text{ABX}_3$  perovskite with bigger A cation occupied in Cubo octahedral position. (a) A cubic  $\text{CH}_3\text{NH}_3\text{PbBr}_3$  perovskite unit cell.<sup>[6]</sup>**

### 1.3 Description of working

Concepts of SCAPS The SCAPS 1D simulator was created by Burgelman et al. Al. Under steady-state

circumstances, solving equations of fundamental semiconductor devices to simulate the electrical properties of thin-film heterojunction solar cells.<sup>[7]</sup> It was employed in this study to investigate the performance of a genuine device (MAPbBr<sub>3</sub>) solar cell with varied material characteristics. The software provides for deep bulk level defect recombination as well as interface defect recombination (non-radiative recombination). Radiative recombination (i.e. direct band-to-band recombination) and interface recombination, which are balanced by Shockley-Read-Hall recombination (propagated by defects or traps), account for a large portion of the recombination losses in the system under consideration. The flow chart below depicts the steps involved while using SCAPS to simulate.

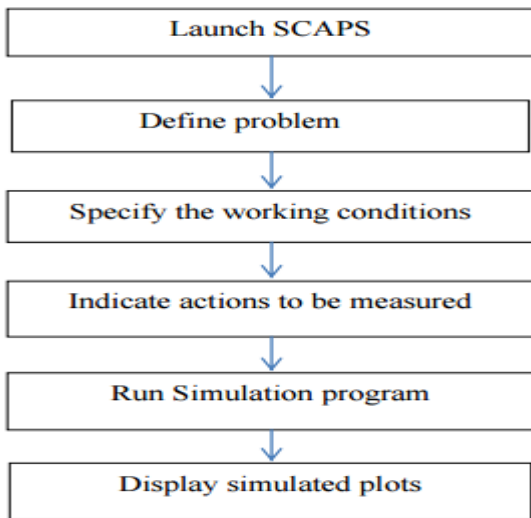


Figure 2: Technique for simulation.

1.4. Simulations Numerical

The term "simulation" refers to the an important approach for gaining a comprehensive understanding of physical activity, the plausibility of proposed physical interpretations, and the impact of physical alterations on the performance of solar cell devices. Solar cells may be simulated using a variety of simulation techniques (SCAPS, AMPS, SCAP, etc). SCAPS (Solar Cell Power Simulator) is a one-dimensional simulation program with seven semiconductor input layers created by a group of solar cell researchers at the University of Ghent's Electronics and Information System Department.<sup>[8]</sup> It is impractical, as well as a waste of effort and money, to construct a solar cell without stimulation. It not only reduces risk, saves time, and money, but it also examines the characteristics layer by layer and how they work to improve the solar cell's efficiency. All of the basic input parameters for simulating a computer should be adequately described in order for it to work as a true equivalent. Perovskite-based solar cells have a different structure than inorganic semiconductor solar cells like CIGS, and perovskite has the interesting form Wannier. As a result, SCAPS may be used to represent perovskite solar cells as a 1D simulator.<sup>[9]</sup>

Table 1: Summary of the basic device equations.<sup>[10]</sup>

Poisson equation	$\frac{\partial}{\partial x}(-\epsilon(x)\frac{d\phi}{dx}) = q [p(x) - n(x) + N_D^+ - N_A^- + P_i(x) - n_i(x)]$
Continuity Equation for electrons	$\frac{\partial n(x,t)}{\partial t} = \frac{1}{q} \frac{\partial J_n}{\partial x} + G_n(x,t) - R_n(x,t)$
Continuity Equation for holes	$\frac{\partial p(x,t)}{\partial t} = \frac{1}{q} \frac{\partial J_p}{\partial x} + G_p(x,t) - R_p(x,t)$
Current density equation for electron	$J_p = q(p\mu_p E - D_p \frac{dp}{dx})$
Current density equation for holes	$J_p = q(p\mu_p E - D_p \frac{dp}{dx})$

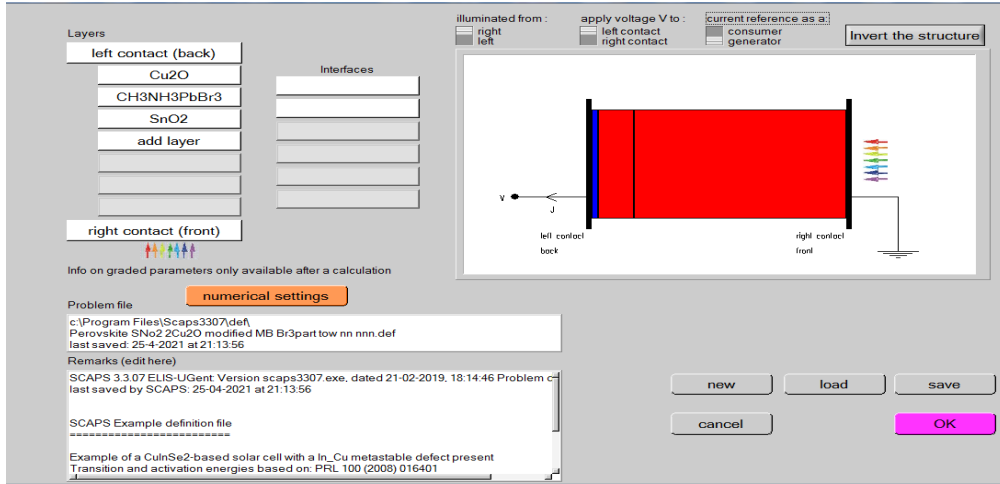


Figure 3: SCAPS panel showing the  $Cu_2O/CH_3NH_3PbBr_3/SnO_2$ .

1.5. SCAPS simulation of  $Cu_2O/Perovskite/SnO_2$

It's worth noting that all simulation settings for each layer in the design were carefully chosen from published

experimental data and other sources.<sup>[11]</sup> Table 2 outlines all of the simulation's major parameters.

Table 2: ETM, absorber, and HTM material qualities.<sup>[12]</sup>

parameters	$Cu_2O$	$CH_3NH_3PbBr_3$	PCBM
Band gap(ev)	2.17	2.33 <sup>[18]</sup>	2.000
Electron affinity (ev)	3.20	3.70 <sup>[19]</sup>	3.900
Dielectric permittivity	7.11	7.50 <sup>[21]</sup>	3.900
CB effective density of states ( $1/cm^3$ )	$2.02E+17$	$1.00+17$ <sup>[21]</sup>	$2.540E+21$
VB effective density of states ( $1/cm^3$ )	$1.10E+19$	$1.00+17$ <sup>[21]</sup>	$2.540E+21$
Electron mobility ( $cm^2/v.s$ )	$2.000E+2$	24 <sup>[22]</sup>	$1.000E+7$
Hole mobility ( $cm^2/v.s$ )	$8.00E+18$	24 <sup>[22]</sup>	$1.000E+7$

Table 3: Devise Parameters use in the numerical analysis.

Right contact electrical properties (Au)	
Thermionic emission /surface recombination	$10^5$
Velocity of electron (cm/s)	
Thermionic emission /surface recombination	$10^7$
Velocity of hole (cm/s)	
Metal (Au) work function (ev)	5.1
Left contact electrical properties	
Thermionic emission /surface recombination	$10^7$
Velocity of electron (cm/s)	
Thermionic emission /surface recombination	$10^5$
Velocity of hole (cm/s)	
the work function of TCO (ev)	4.4

DISCUSSION AND CONCLUSION

1- On the  $Cu_2O/CH_3NH_3PbBr_3/PCBM$  solar cells, the effect of layer thickness, temperature, defects, and work function change

1.1- The impact of the thickness of the  $CH_3NH_3PbBr_3$   
To absorb the most photons and form electron-hole pairs, the absorber layer should be adjusted to the optimal thickness. The thickness of the absorber layer has been changed from 0.03m to 0.09m. The longer wavelength of the light will result in a significant quantity of electron-hole pair creation as the thickness of the absorber layer

grows. The depletion layer becomes extremely similar to the back contact when the absorber layer thickness is increased, The rear contact collects even more electrons for recombination. As a result, the producing process will consume fewer electrons, resulting in a lower filling factor and reduced efficiency. Variation in PV characteristics as a function of absorber layer thickness is seen in Figure 4.

**Table 4: Variation of Thickness for CH<sub>3</sub>NH<sub>3</sub>PbBr<sub>3</sub> with device parameters.**

Thickness(μm) CH <sub>3</sub> NH <sub>3</sub> PbBr <sub>3</sub>	V <sub>OC</sub> (V)	J <sub>sc</sub> (mA/cm <sup>2</sup> )	F.F (%)	η (%)
0.03	3.66	36.84	11	14.86
0.04	3.36	36.68	10.30	12.72
0.05	2.87	36.49	10.16	10.85
0.06	2.46	36.24	9.71	8.68
0.07	2.17	35.88	8.77	6.84
0.08	1.96	35.20	7.49	5.18
0.09	1.81	33.74	6.12	3.74

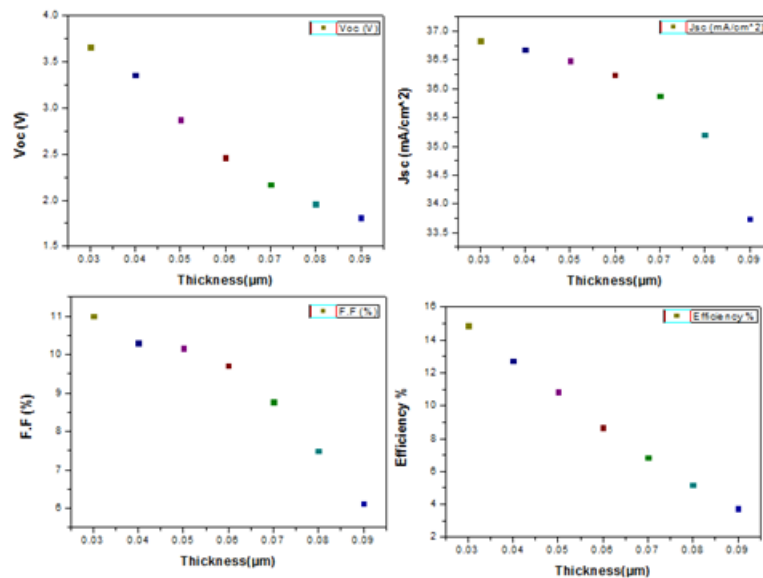


**Figure 4. Variation of PV parameters by varying the thickness of CH<sub>3</sub>NH<sub>3</sub>PbBr<sub>3</sub>.**

**1.2-Effect of the PCBM (ETL) thickness change on solar cells.**

The ETL thickness was adjusted from (0.05) to (0.19)m. With a larger PCBM thickness, the longer wavelength of light allows for more electron-hole pair generation. The thickness of the PCBM layer of PV parameters varies as stated in table (18). Voc is stable, whereas Jsc and usually fall (45.48 to 45.05) and (63.95 to 64.05) percent, respectively. FF rises from 63.95 to 64.05 percent on

average. As the absorber layer thickness increases, the longer wavelength of light will produce a large number of electron-hole pairs. As the thickness of the absorber layer is lowered, the depletion layer becomes more close to the back contact, allowing more electrons to be trapped by the back contact for recombination. As a result, at the thickness of 0.15 m, fewer electrons will participate in the producing process, resulting in poorer efficiency and a fall in FF.

**Table (5): Shows the drawing data for variation thickness of PCBM.**

Thickness(μm)	Voc (V)	Jsc (mA/cm <sup>2</sup> )	F.F (%)	η (%)
0.05	1.08	45.48	63.95	31.53
0.07	1.08	45.36	64.04	31.49
0.09	1.08	45.27	64.05	31.43
0.11	1.08	45.21	64.06	31.39
0.13	1.08	45.51	64.06	31.53
0.15	1.08	45.11	64.05	31.32
0.17	1.08	45.08	64.05	31.29
0.19	1.08	45.05	64.05	31.27

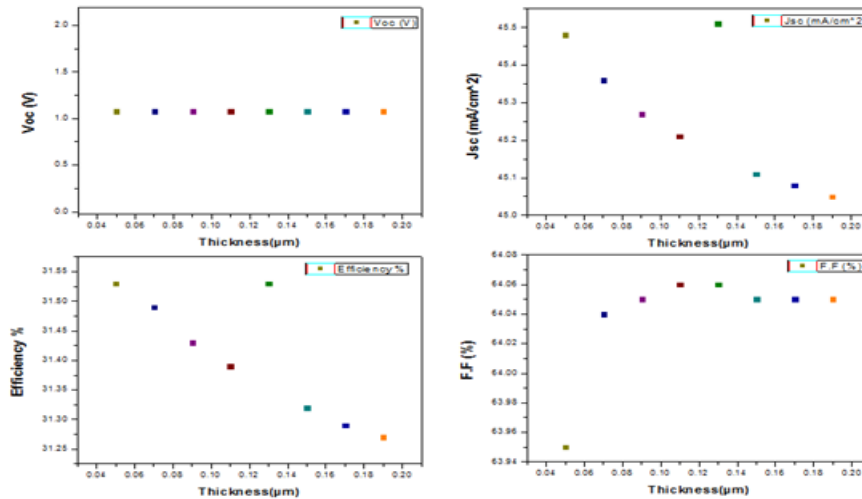


Figure (5): Variation of PV parameters by varying the thickness of PCBM.

**1.3-Effects of the CB,VB density of State of the(Cu<sub>2</sub>O/CH<sub>3</sub>NH<sub>3</sub>PbBr<sub>3</sub>/PCBM).**

When the DOS CB is increased from (1\*10<sup>16</sup> to 1\*10<sup>20</sup>)cm<sup>-3</sup>, all of the device's properties stay unaltered. When increasing (1\*10<sup>12</sup> to 1\*10<sup>22</sup>) cm<sup>-3</sup> Voc while

reducing (1.09 to 1.08) volts and (30.15 to 30.49) percent in VB. From (63.48 to 64.40) percent, (45.84 to 43.77) (mA/cm<sup>2</sup>), FF and Jsc typically rise. When the CB is increased, all of the device's settings stay constant. as seen in table 6.

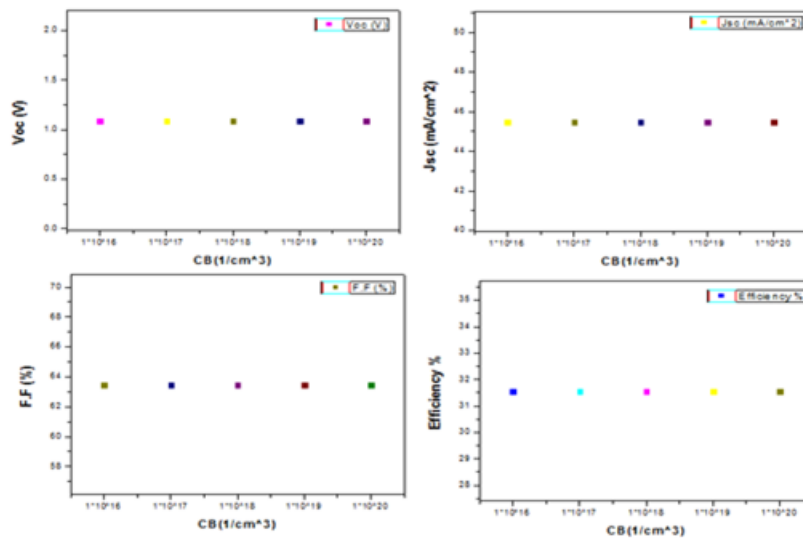


Table 6: Variation of CB for Cu<sub>2</sub>O/ CH<sub>3</sub>NH<sub>3</sub>PbBr<sub>3</sub>/PCBMwith device parameters.

CB (1/cm <sup>3</sup> )	Voc (V)	Jsc (mA/cm <sup>2</sup> )	F.F (%)	η (%)
1*10 <sup>16</sup>	1.09	45.48	63.47	31.56
1*10 <sup>17</sup>	1.09	45.48	63.47	31.56
1*10 <sup>18</sup>	1.09	45.48	63.47	31.56
1*10 <sup>19</sup>	1.09	45.48	63.47	31.56
1*10 <sup>20</sup>	1.09	45.48	63.47	31.56

Table 7: Variation of VB for Cu<sub>2</sub>O/ CH<sub>3</sub>NH<sub>3</sub>PbBr<sub>3</sub>/PCBM with device parameters.

VB (1/cm <sup>3</sup> )	Voc (V)	Jsc (mA/cm <sup>2</sup> )	F.F (%)	η (%)
1*10 <sup>12</sup>	1.09	45.84	63.48	32.15
1*10 <sup>14</sup>	1.09	46.83	63.48	32.13
1*10 <sup>16</sup>	1.09	45.48	63.50	31.56
1*10 <sup>18</sup>	1.08	44.97	63.11	30.71
1*10 <sup>20</sup>	1.08	44.52	63.32	30.5
1*10 <sup>22</sup>	1.08	43.77	64.40	30.49

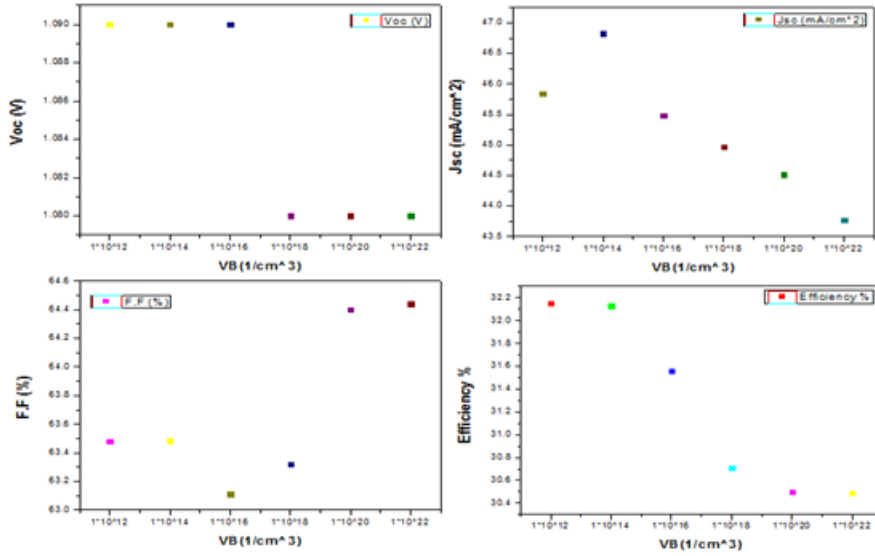


Figure 7: VB density of the Cu<sub>2</sub>O/CH<sub>3</sub>NH<sub>3</sub>PbBr<sub>3</sub>/PCBM layer.

**1.4- Effect of annealing Temperatures for CH<sub>3</sub>NH<sub>3</sub>PbBr<sub>3</sub>**

Temperatures have a significant impact on the device characteristics. In the PCBM material, we see that as the temperature rises, the efficiency, current, and voltage rise, but the filling factor falls. The fact that efficiency increases with temperature shows that this material can

withstand high temperatures. Temperatures ranged from 213 to 333 degrees Celsius. At achieve the best results, the model's operating temperature is set to 213K. According to tabl 21, the model's best possible efficiency at this temperature is 35.38 percent, with a fill factor of 69.62 percent, Jsc = 45.93mA/cm<sup>2</sup>, and Voc=1.1V.

Table 8: The parameter of the Cu<sub>2</sub>O/CH<sub>3</sub>NH<sub>3</sub>PbBr<sub>3</sub>/SnO<sub>2</sub> heterojunction solar cells.

T(K)	Voc (V)	Jsc (mA/cm <sup>2</sup> )	F.F (%)	η (%)
213	1.1	45.93	69.62	35.38
233	1.11	45.93	69.06	35.27
253	1.11	45.93	68.5	34.96
273	1.10	45.93	67.52	34.34
293	1.10	45.93	66.76	33.33
313	1.10	45.92	62.74	31.74
333	1.10	45.92	58.25	29.64

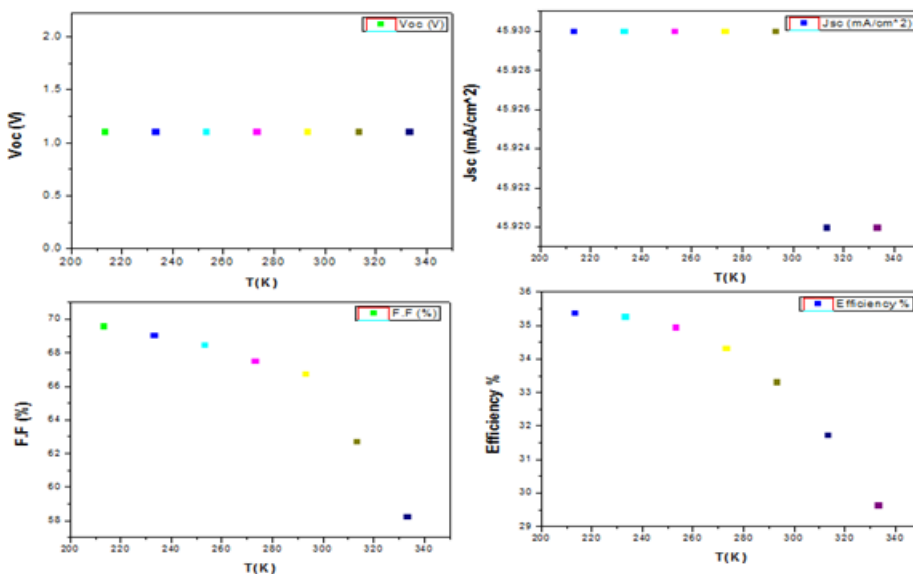


Figure-8: Variation of solar cell parameters with the Operating temperature.

## CONCLUSIONS

The efficiency of the structure  $\text{Cu}_2\text{O}/\text{CH}_3\text{NH}_3\text{PbBr}_3/\text{PCBM}$  device was examined at various temperatures, defects, and work functions in order to discover the optimal condition corresponding to the maximum efficiency of the structure  $\text{Cu}_2\text{O}/\text{CH}_3\text{NH}_3\text{PbBr}_3/\text{PCBM}$  device, which was 35.38 percent at 213K.

## REFERENCE

1. Y. Wang *et al.*, "Solvent annealing of PbI<sub>2</sub> for the high-quality crystallization of perovskite films for solar cells with efficiencies exceeding 18%," *Nanoscale*, 2016; 8(47): 19654–19661.
2. N. Mahani, "Pseudo-System-Level Network-on-Chip Design and Simulation with VHDL: A Comparative Case Study on Simulation Time Trade-Offs," *Indian J. Sci. Technol.*, 2016; 9(7).
3. U. Mandadapu, S. V. Vedanayakam, K. Thyagarajan, M. R. Reddy, and B. J. Babu, "Design and simulation of high efficiency tin halide perovskite solar cell," *Int. J. Renew. Energy Res.*, 2017; 7(4): 1603–1612.
4. V. M. Goldschmidt, "Crystal structure and chemical correlation," *Ber Deut Chem Ges*, 1927; 60: 1263–1296.
5. M. Rini *et al.*, "Control of the electronic phase of a manganite by mode-selective vibrational excitation," *Nature*, 2007; 449: 72–74.
6. G. Giorgi, J.-I. Fujisawa, H. Segawa, and K. Yamashita, "Small photocarrier effective masses featuring ambipolar transport in methylammonium lead iodide perovskite: a density functional analysis," *J. Phys. Chem. Lett.*, 2013; 4(24): 4213–4216.
7. A. Slami, M. Bouchaour, and L. Merad, "Numerical study of based perovskite solar cells by SCAPS-1D," *Int. J. Energy Environ.*, 2019; 13: 17–21.
8. A. Niemegeers, M. Burgelman, and K. Decock, "SCAPS Manual. University of Gent." Go to reference in article, 2014.
9. A. Niemegeers, M. Burgelman, K. Decock, J. Verschraegen, and S. Degraeve, "SCAPS manual," *Univ. Gent*, 2014; 13.
10. T. L. Amu, "Performance optimization of tin halide perovskite solar cells via numerical simulation, 2014.
11. M. I. Hossain, F. H. Alharbi, and N. Tabet, "Copper oxide as inorganic hole transport material for lead halide perovskite based solar cells," *Sol. Energy*, 2015; 120: 370–380.
12. N. K. Noel *et al.*, "Lead-free organic–inorganic tin halide perovskites for photovoltaic applications," *Energy Environ. Sci.*, 2014; 7(9): 3061–3068.